Progress of Theoretical Physics, Vol. 99, No. 6, June 1998

Time-Reversal Symmetry Breaking States in High-Temperature Superconductors

Manfred SIGRIST

Yukawa Institute for Theoretical Physics, Kyoto University, Kyoto 606-8502, Japan

(Received February 18, 1998)

The $d_{x^2-y^2}$-wave symmetry of the order parameter leads to various physical phenomena of high-temperature superconductors which are not present in standard superconductors. A particularly interesting new aspect occurs in connection with the behavior of the order parameter in the vicinity of interfaces (Josephson junctions) between superconductors and close to surfaces. In this review we discuss the appearance of localized states with broken time-reversal symmetry in these regions, using various different schemes of analysis: the tunneling formalism, the Bogolyubov-de Gennes equation, and the generalized Ginzburg-Landau theory. We demonstrate that this kind of state is connected with the opening of a gap in the quasiparticle density of states which lowers the local free energy density. A direct consequence of time-reversal symmetry breaking can be seen in the presence of spontaneous supercurrents. Other features, such as the possibility of vortices with fractional flux quanta and unusual phase slip effects in Josephson junctions are examined as possible experimental indications for a time-reversal symmetry breaking state. Furthermore, quasiparticle tunneling has been recently discussed and applied to probe the surface of such a superconductor for the violation of time-reversal symmetry. Concerning the magnetic properties surfaces supporting such a state can yield a paramagnetic contribution to the magnetic response of the superconductor. Finally, some examples of superconductors which break time-reversal symmetry in the bulk are discussed. Clear signals in the zero-field relaxation rate of muons leave little doubt that such superconducting states are realized in UPt_3, $U_{1-x}Th_xBe_{13}$ and Sr_2RuO_4.

§1. Introduction

The surprising discovery of superconductivity in CuO_2-materials had a dramatic impact on the focus of research in condensed matter physics.[1] It was not only the high transition temperatures but also various other unusual properties of this new class of materials which attracted the interest of many researchers during the last decade. Despite of much progress, still there is the unresolved mystery: how does the unusual metallic state which yields superconductivity emerge out of a magnetic insulator upon relatively moderate doping with carriers?[2] It is a challenging problem for theoretical physics to explain the rich structure of the phase diagram which is basically common to all high-temperature superconductors. Considerable effort has been invested into the search for the mechanism causing superconductivity. There is little doubt that the superconducting state is a result of Cooper pairing common to all known superconductors. The pairing symmetry, however, could be unconventional due to strong correlation effects and mechanisms other than the standard one based on the electron-phonon interaction.

It has become one of the important issues during the last four years to determine the symmetry of the Cooper pairs in the hope that it may provide a hint about the

underlying mechanism.[3),4)] Today a great deal of experimental data give convincing evidence that the pair wavefunction has $d_{x^2-y^2}$-wave character, most commonly written as

$$\psi(\boldsymbol{k}) = \langle c^\dagger_{\boldsymbol{k}\uparrow} c^\dagger_{-\boldsymbol{k}\downarrow} \rangle \propto \cos k_x - \cos k_y, \tag{1·1}$$

where $c^\dagger_{\boldsymbol{k}s}$ denotes the electron creation operator. Nevertheless, the mechanism remains a matter hotly debated among various groups. Pairing with $d_{x^2-y^2}$-wave symmetry is a property common to several theories. One such theory is based on the idea that the pairing interaction is mediated through the exchange of antiferromagnetic spin fluctuations among the quasiparticles.[5),6)] Another describes the superconducting states as pairing resulting from the doping of a spin liquid state, the so-called resonating valence bond (RVB) state.[7)-9)] An alternative view presented recently proposes the existence of a large continuous symmetry $SO(5)$ which establishes a connection between the antiferromagnetic and the superconducting order parameters.[10)] These competing scenarios in addition to others are still a matter of controversy.

It is not the goal of this article to elaborate on these microscopic theories further. Rather, we would like to give here a review of some implications of d-wave pairing in high-temperature superconductors, in particular, in connection with the internal phase structure of the pair wave function (Eq. (1·1)). The phenomena best investigated theoretically, as well as experimentally, in this respect are related with the Josephson effect, which provides a very powerful means to study the phase of the superconducting order parameters.[11),12)] The Josephson effect turned out to be crucial in the experimental tests of the pairing symmetry, because it allows for the detection of the sign difference in the pair wave function along the x- and y-coordinate. The presence of nodes in the quasiparticle excitation gap seen by number of other important experiments are in this respect less decisive for the identification of the pairing symmetry, because this feature is shared by various pairing states.[3),4)]

This article is mainly concerned with the possibility of order parameter configurations which break time-reversal symmetry, for example on certain Josephson junctions, at surfaces or other inhomogeneities. We show that such states can lead to unusual magnetic properties. The possibility of time-reversal symmetry breaking superconducting states is not unlikely in view of the strong evidence for such states in the heavy Fermion superconductors UPt_3 and $U_{1-x}Th_xBe_{13}$ and the more recently discovered compound Sr_2RuO_4, as we discuss in the last section.

§2. Order parameter symmetry

All high-temperature superconductors consist of CuO_2-planes stacked on top of each other and separated by layers of other elements. The prevailing view is that the physics essential to the superconductivity occurs in these CuO_2-planes, while the intermediate layers act as charge reservoirs to remove or add electrons to the planes. Therefore the discussion of the symmetry of the superconducting

state must be based on the lattice structure of the planes, which is basically square-like (with a slight orthorhombic distortion in some cases). The pairing states in this lattice should be classified according to the irreducible representations of the square lattice point group C_{4v} analogous to the angular momentum classification in a rotationally symmetric system.[13] These representations include both even- (spin singlet) and odd-parity (spin triplet) pairing states. It is possible to distinguish the two states by some of their magnetic properties. For spin singlet pairing, the spin susceptibility is suppressed in the superconducting state, while it should be only weakly affected for spin triplet states, since in the latter the spin degrees of freedom remain active. In measurements of the Knight shift Barrett and coworkers demonstrated that spin triplet pairing can be ruled out.[14] Thus we restrict the even-parity representations which consist of four one-dimensional (A_{1g}, A_{2g}, B_{1g} and B_{2g}) and a two-dimensional (E_g) representation. We ignore the last one, because it would imply interlayer pairing and is, for this reason, a rather unlikely candidate. The list of the remaining pairing states is given in Table I, with their symmetry structures illustrated in Fig. 1. The pair wave functions are given in momentum space corresponding to real space pairing of particles on nearest or next nearest neighbor sites. A constraint for the form of the pair wave function is imposed by the strong Coulomb repulsion among the carriers in the CuO_2-plane, which forbids them to occupy the same site. Therefore any onsite pairing amplitude has to vanish in the pair wave function, leading to the condition

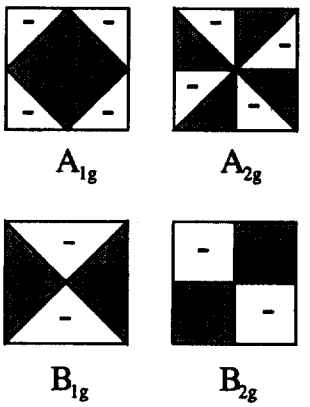

Fig. 1. Schematic view of the symmetry of the four possible pairing states on the square lattice.

$$0 = \langle c_{i\uparrow}^{\dagger} c_{i\downarrow}^{\dagger} \rangle = \frac{1}{N} \sum_{\boldsymbol{k}} \langle c_{\boldsymbol{k}\uparrow}^{\dagger} c_{-\boldsymbol{k}\downarrow}^{\dagger} \rangle = \frac{1}{N} \sum_{\boldsymbol{k}} \psi(\boldsymbol{k}), \tag{2·1}$$

where the sum runs over the momenta in the first Brillouin zone of the square lattice. The most symmetric state in the A_{1g} representation cannot be a genuine (structureless) "s-wave" pairing state, but has the form of a so-called "extended s-wave" state, which has nodes in the first Brillouin zone in order to satisfy Eq. (2·1). There are two pair wave functions, usually called the $d_{x^2-y^2}$-wave and d_{xy}-wave in B_{1g} and B_{2g}, respectively. Finally, the state belonging to A_{2g} has a more complicated nodal structure and might be termed "g-wave".

All four symmetries are equally good candidates for the superconducting states in the CuO_2-plane from group theoretical point of view. Finally, only the experiments or a microscopic theory can decide which among them is realized. A number of experiments including the above mentioned Knight shift measurement[14] indicate low-lying quasiparticle excitations which require nodes in the gap.[3] This is satisfied by all four states. To reduce the number of candidates information regarding the

position of the nodes in momentum space would be definitely helpful. This has been done successfully by angle resolved photoemission spectroscopy (ARPES), which locates the nodes exclusively along the [110]-direction in $Bi_2Sr_2CaCu_2O_8$ (BSCCO) and $YBa_2Cu_3O_7$ (YBCO).[15] This rules out A_{2g} and B_{2g}, while B_{1g} is the strongest candidate, while A_{1g} is still possible.

Table I. Symmetry classification of the even-parity pairing states.

Γ	$\psi(\boldsymbol{k})$
A_{1g}	$\cos k_x + \cos k_y$
A_{2g}	$\sin k_x \sin k_y (\cos k_x - \cos k_y)$
B_{1g}	$\cos k_x - \cos k_y$
B_{2g}	$\sin k_x \sin k_y$
E_g	-

Decisive information on the symmetry of the pair wave function came finally from phase sensitive probes such as the Josephson effect which identified the symmetry as the $d_{x^2-y^2}$-wave (B_{1g}) for all of the HTSC tested to this time. These probes consider the internal phase structure of the pair wave function. It is important to know how the wave function transforms under all point symmetry elements of the crystal lattice (C_{4v}), as given in Table II. The order parameter η of the superconducting state given by

$$\Psi(\boldsymbol{r}, T, \boldsymbol{k}) = \eta(\boldsymbol{r}, T)\psi(\boldsymbol{k}) \tag{2·2}$$

is a complex function of position and temperature, which transforms according to Table II ($\eta = |\eta| e^{i\phi}$). This information enters into the discussion of the Josephson effect given in the next section.

§3. The Josephson effect

If two superconductors (A and B) are brought into contact, so that Cooper pairs can tunnel between them, then the two corresponding order parameters, η_A and η_B (in particular their phases) are no longer independent. In standard superconductors, the two phases are equal in the lowest energy configuration of the superconductors. A finite phase difference leads, in general, to supercurrents flowing through the interface. This is the Josephson effect, and to lowest order in the coupling, the current can be expressed by

Table II. Symmetry properties of the B_{1g} state.

g	E	$2C_4$	C_2	σ	σ'
sign($\psi(\boldsymbol{k})$)	+1	−1	+1	+1	−1

$$I = I_0 i(\eta_A^* \eta_B - \eta_A \eta_B^*) = I_c \sin(\phi_B - \phi_A), \tag{3·1}$$

which is the Josephson current-phase relation between the superconductors A and B with the order parameters η_A and η_B at the interface. The critical current $I_c = 2I_0|\eta_A||\eta_B|$ depends on the coupling constant I_0 as well as the temperature dependent order parameters. The junction energy corresponds to the lowest order coupling of the two superconductors,

$$E_J = -\frac{I_0 \Phi_0}{2\pi c}(\eta_A^* \eta_B + \eta_A \eta_B^*) = -\frac{I_c \Phi_0}{2\pi c} \cos(\phi_B - \phi_A). \tag{3·2}$$

This somewhat simplified expression for the current-phase relation allows us to understand rather easily the implication of the internal phase structure of the order parameter for the Josephson effect.[17),18),22)] Consider the situation in which we couple a standard s-wave to a $d_{x^2-y^2}$-wave superconductor, as shown in Fig. 2. For Josephson tunneling, the orientation of the d-wave superconductor enters as an important aspect, because it is a direction sensitive effect. This can be seen immediately through the operation of certain elements of C_{4v} on the $d_{x^2-y^2}$-wave superconductor (Table II). Let us consider the behavior of the current I for a given angle θ under some of these elements, where θ is the relative angle of one of the main axes to the interface normal vector. The d-wave nature of the order parameter implies the following three relations concerning I for different, but related angles:

$$\begin{aligned} I(-\theta) &= +I(\theta), \\ I(\theta \pm \frac{\pi}{2}) &= -I(\theta), \\ I(\theta \pm \pi) &= +I(\theta) \end{aligned} \tag{3·3}$$

for an arbitrary phase difference $\varphi = \phi_B - \phi_A$.[12),19)-21)] Thus we may consider the critical current as a θ-dependent function $I(\theta)$. The most simple form generating the above relations is $I_c = I_{c0}\cos(2\theta)$. This form certainly does not reproduce the angular dependence of the coupling strength correctly, but merely gives the proper sign structure. The general form would be

$$I_c(\theta) = \sum_{m=0}^{\infty} I_{cm}\cos((4m+2)\theta) \tag{3·4}$$

which, unfortunately, contains an inconveniently large number of parameters I_{cm} and information unnecessary for the following discussions. Thus in the following we consider only the simple form of $I_c(\theta)$.

The sign of $I_c(\theta)$ can also be absorbed into an intrinsic phase shift α of the junction, which is $\alpha = 0$ for $I_c > 0$ and $\alpha = \pi$ for $I_c < 0$. Obviously, this definition is not unique, because $\theta = 0$ is not uniquely defined for a square lattice — the choice of the "x"- and "y"-main axes is arbitrary. Despite this "gauge" freedom for α, the notion of a "0-" and "π-junction" corresponding to the phase shift α is a useful concept in many respects.

The presence of intrinsic phase shifts $\alpha = \pi$ can lead to various unusual properties in multiply connected systems.[12)] In particular, interference phenomena were used to prove the existence of π-phase shifts in a number of HTSC, identifying the order parameter symmetry as $d_{x^2-y^2}$-wave like.[31),23)-28)] It was also shown that a π-phase shift in

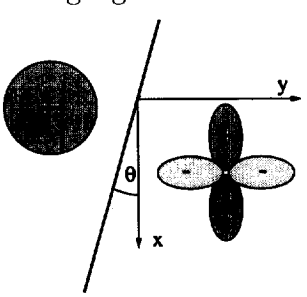

Fig. 2. Interface between an s- and a $d_{x^2-y^2}$-wave superconductor.

a superconducting loop made of several connected grains of a d-wave superconductor lead to a new type of flux quantization, namely half-integer quantization in units of $\Phi_0 = hc/2e$.[11),12)] Remarkably, this leads to a doubly degenerate lowest energy state of the loop with a finite spontaneous current.[12)] This property is the basis of one of the most beautiful test experiments for the d-wave character of the HTSC.[29),30)] We do not go into further detail here and refer the reader to a number of reviews on this topic.[3),4),31)]

§4. The intrinsic phase shifts

The phase shift α determines the minimum of the junction energy

$$E_{J,\alpha}(\varphi) = -\frac{|I_c|\Phi_0}{2\pi c}\cos(\varphi - \alpha), \tag{4·1}$$

which lies at the phase difference $\varphi = \alpha$. Let us now assume a specific gauge where θ is defined and $\alpha(\theta = 0) = 0$. Then we may ask how α changes if we rotate the angle θ from 0 to $\pi/2$. The definition of α in the previous section would imply a discontinuous change of α from 0 to π at $\theta = \pi/4$. On the other hand, it might be possible that α changes continuously between the two limiting values in the vicinity of $\theta = \pi/4$, as indicated in Fig. 3. This question cannot be answered within the above description based on lowest order coupling. A more careful analysis of the physics of the interface is necessary.

Before going into details on how a continuous variation of α might occur, we would like to consider the interpretation of $\alpha \neq 0, \pi$. For this purpose we first analyze the energy $E_{J,\alpha}$ in Eq. (4·1) for the lowest order coupling. Obviously, $E_{J,\alpha}(\varphi) = E_{J,\alpha}(\varphi + 2\pi n) = E_{J,\alpha+2\pi m}(\varphi)$ for any integers m and n. If we apply the time-reversal operation, then $\eta_{A,B} \to \eta^*_{A,B}$. This results in

$$\varphi \to -\varphi \qquad \text{and} \qquad \alpha \to -\alpha \tag{4·2}$$

which is naturally connected with the reversal of the Josephson current. If $\alpha = 0$ or π then $E_{J,\alpha}$ and $E_{J,-\alpha}$ describe identical Josephson junctions. In particular, the lowest energy state is located at the same value of φ which is non-degenerate, apart from the addition of integer multiples of 2π. On the other hand, for $\alpha \neq 0, \pi$ the time-reversed junction has a different lowest energy state ($-\alpha \neq \alpha + 2\pi m$). The degeneracy of this junction is two-fold. The junction breaks time-reversal symmetry, because the lowest energy state is not unique, but changes under time reversal.

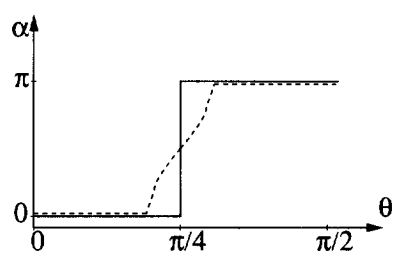

Fig. 3. The phase shift α versus the angle θ. The phase shift can change discontinuously (solid line) or continuously (dashed line) between the two values 0 and π close to $\theta = \pi/4$.

The broken time-reversal symmetry of Josephson junctions definitely appears if at least one of the two connected superconductors breaks time-

reversal symmetry. In order to break time reversal symmetry, at least two order parameter components which must be combined with complex coefficients are necessary. Thus, we have to add a further component of different symmetry to the $d_{x^2-y^2}$-wave order parameter. This order parameter η' can correspond to the extended s-wave (A_{1g}) pairing state or the d_{xy}-wave state (B_{2g}). Time-reversal symmetry is broken for a combination of η and η' if

$$\eta + \eta' \to \eta^* + \eta'^* \neq (\eta + \eta')e^{i\gamma} \tag{4·3}$$

i.e., $\eta+\eta'$ and its time-reversed $\eta^*+\eta'^*$ are different, but degenerate states. This is the case if the relative phase $\phi-\phi' \neq 0, \pi$ ($\eta = |\eta|e^{i\phi}$ and $\eta' = |\eta'|e^{i\phi'}$). Two time-reversal symmetry breaking states were proposed in the context of HTSC, the "$s + id$-wave" and the "$d + id'$-wave" state both with $\phi - \phi' = \pm\pi/2$. The corresponding gap functions in the quasiparticle spectrum,

$$\Delta(\boldsymbol{k}) = \sqrt{|\eta\psi_d(\boldsymbol{k}) + \eta'\psi'(\boldsymbol{k})|^2}, \tag{4·4}$$

are nodeless in both cases. The experimentally observed nodes, however, ruled out such a time-reversal breaking states in most of the HTSC.

For the moment we assume, however, that the superconductor B violates time reversal symmetry, described by the two-component order parameter (η_B, η'_B). The intrinsic phase shift can be obtained from the study of the junction energy,[17),22)]

$$\begin{aligned} E_J &= -E_0[(\eta_A^*\eta_B + \eta_A\eta_B^*) + (\eta_A^*\eta'_B + \eta_A\eta'^*_B)] \\ &= -E_0[|\eta_A||\eta_B|\cos(\phi_B - \phi_A) + |\eta_A||\eta_B|\cos(\phi'_B - \phi_A)] \\ &= -E_0|\eta_A|\sqrt{(|\eta_B| + |\eta'_B|\cos\chi)^2 + |\eta'_B|^2\sin^2\chi}\cos(\varphi - \alpha), \end{aligned} \tag{4·5}$$

where $E_0 = I_0\Phi_0/2\pi c$, $\varphi = \phi_B - \phi_A$, $\chi = \phi_B - \phi'_B$ and

$$\tan\alpha = \frac{|\eta'_B|\sin\chi}{|\eta| + |\eta'|\cos\chi}. \tag{4·6}$$

Note that the phase shift satisfies $\alpha \neq 0, \pi$ if the relative phase $\chi \neq 0, \pi$, i.e. for time-reversal symmetry breaking states.[32),33)] In the following sections we examine the situation in which time-reversal symmetry is conserved in the bulk, but is violated locally at the Josephson junction.

§5. Broken time-reversal symmetry on the Josephson junction

We consider here three ways of describing the occurrence of intermediate values for the phase shift α. The first view is based on multiple Cooper pair transfer through the Josephson junction. The second addresses the arrangement of Andreev bound states in the contact, and the third considers the proximity effect between the two superconductors. In essence all three methods express slightly different aspects of the same physics. For the sake of transparency we keep the technical discussion at a low level, while emphasizing the physical interpretation.

5.1. *Multiple Cooper pair transfer*

The current-phase relation in Eq. (3·1) includes only the lowest order contribution to the Josephson effect when only the transfer of single Cooper pairs are considered. Higher order corrections can lead to important modifications for d-wave superconductors, as was shown by Yip.[21),34)] To illustrate in particular the effect on the intrinsic phase shift α, we start with a simple extension of the current-phase relation which includes second-order contributions (i.e., simultaneous tunneling of two pairs),

$$I(\varphi) = I_1 \sin\varphi + I_2 \sin 2\varphi \tag{5·1}$$

and for the free energy

$$F_J(\varphi) = -\frac{\Phi_0}{2\pi c}[I_1 \cos\varphi + I_2 \cos^2\varphi] + \text{const.} \tag{5·2}$$

The lowest energy state has to satisfy $\frac{dF_J}{d\varphi}|_{\varphi=\varphi_0} \propto I(\varphi_0) = 0$. This leads to

$$\sin\varphi_0 = 0 \qquad \text{or} \qquad \cos\varphi_0 = -\frac{I_1}{2I_2}, \tag{5·3}$$

which yields a minimum for

$$\varphi_0 = \begin{cases} 0 & \text{for} \quad I_1 > 0, \\ \pi & \text{for} \quad I_1 < 0 \end{cases} \tag{5·4}$$

if $|I_1/2I_2| > 1$ and

$$\varphi_0 = \pm\arccos(-I_1/2I_2) \tag{5·5}$$

for $I_2 < 0$ and $|I_1/2I_2| < 1$. The intrinsic phase shift is $\alpha = \varphi_0$. Obviously, the second solution (Eq. (5·5)) corresponds to a two-fold degenerate state which breaks time-reversal symmetry according to our previous definition.

It is important now to show that conditions for the second solution in Eq. (5·5) can indeed be satisfied in a Josephson junction. We again look at the junctions geometry given in Fig. 2. On a microscopic level, multiple Cooper pair transfers between the two superconductors can be described using the Bogolyubov-de Gennes equations or doing a quasiclassical approach.[36)-38)] The interface shall be represented by a simple potential barrier, $\mathcal{H}_{\text{barr}} = Z\delta(x)$. Then the current density has the form

$$j(\varphi) = \frac{e}{\pi\hbar}\int_{-\pi/2}^{\pi/2} d\vartheta \frac{1}{\beta}\sum_{\omega_n} \frac{t(\vartheta)\Delta_A\Delta_B(\vartheta-\theta)\sin\varphi}{[\omega_n^2 + \Delta_A\Delta_B(\vartheta-\theta)\cos\varphi + E_{nA}E_{nB}]t(\vartheta) + ZE_{nA}E_{nB}}, \tag{5·6}$$

where for simplicity we restrict the angle integral over ϑ on the basal plane of the d-wave superconductor (the c-axis is always parallel to the interface).[21),39)] The function $t(\vartheta)$ denotes the tunneling form factor of the junction. With the simple choice $t(\vartheta) = t_0 \cos^2\vartheta$, we favor perpendicular tunneling. Furthermore, Δ_A denotes

the s-wave gap and $\Delta_B(\vartheta)$ the angle-dependent d-wave gap with $\Delta_B(\vartheta) = \Delta_0 \cos 2\vartheta$. The corresponding quasiparticle energies are $E_n = [\omega_n^2 + \Delta^2]^{1/2}$ where $\omega_n = \pi(2n+1)/\beta$ is the Matsubara frequency ($\beta^{-1} = k_B T$). In the limit $Z \gg 1$, Eq. (5·6) reduces to the Ambegaokar-Baratoff form to lowest order, which is obtained from a tunneling Hamiltonian description.[35] In this limit it is also possible to expand Eq. (5·6) in $\Delta_A \Delta_B$:

$$j(\varphi) = \frac{e}{\pi\hbar} \int_{\pi/2}^{\pi/2} d\vartheta \frac{1}{\beta} \sum_{\omega_n} \frac{\Delta_A \Delta_B(\vartheta - \theta) t(\vartheta) \sin\varphi}{(\omega_n^2 + E_{nA} E_{nB}) t(\vartheta) + Z E_{nA} E_{nB}} \times \left(1 - \frac{\Delta_A \Delta_B(\vartheta - \theta) t(\vartheta) \cos\varphi}{(\omega_n^2 + E_{nA} E_{nB}) t(\vartheta) + Z E_{nA} E_{nB}}\right) + \cdots . \tag{5·7}$$

The sign of the second term is negative, as is necessary for the non-trivial solution Eq. (5·5). This second order term also represents the feedback effect of the ϕ-dependence of the interface energy on the Josephson current. In other words, a finite current enhances the energy, which in turn tends to decrease the current for given phase difference ϕ. This aspect of the tunneling formulation is common to the Josephson effect between superconductors of any symmetry and is not specific to the above configuration of an s- and a d-wave superconductor.

The first term, proportional to Δ^2 vanishes more slowly than the second, proportional to Δ^4 as the temperature approaches T_c from the superconducting side. Therefore the condition $|I_1| < -2I_2$ is satisfied for lower temperatures. For the specific case $\theta = \pi/4$ the first term disappears for any temperature so that $\alpha = \pm\pi/2$ minimizes the junction energy for all $T < T_c$ — a feature specific to the $d_{x^2-y^2}$-wave superconductor. For general angles, however, there is a critical $\tilde{T}_c$ below which the phase shift α deviates continuously from 0 or π.[21] Thus, we may consider this change at $\tilde{T}_c$ as a second order phase transition of the Josephson junction, breaking time-reversal symmetry. From this formulation we obtain a phase diagram of temperature versus θ, as given in Fig. 4. With lowering temperature, the range occupied by the new junction state around $\theta = \pi/4$ grows. The location of the transition line depends on various parameters, such as the magnitude of tunneling barrier Z, the tunneling form factor $t(\vartheta)$ and, of course, on the specific temperature dependence of the gaps $\Delta_{A,B}$. The schematic phase diagram in Fig. 4 agrees on a qualitative level with those of all the following treatments. This theory does not attempt to describe the detailed structure of the order parameter in and close to the inter-

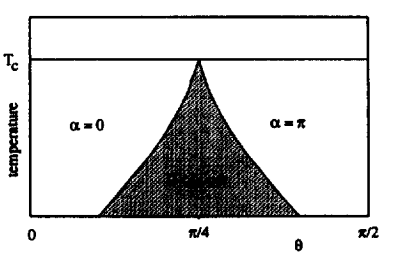

Fig. 4. Schematic phase diagram for temperature versus the angle θ. In the shaded region the phase shift α takes intermediate values so that the junction breaks time-reversal symmetry. This region grows with lowering temperature.

face. In particular, there is no region where the s- and d-wave order parameters coexist and combine to a time-reversal symmetry breaking state, as we will find in the next two subsections. These features are included effectively in the interface parameters, Z and $t(\vartheta)$, and would be obtained if we integrated out all degrees of freedom, apart from the order parameter phases. Therefore, the only remaining feature is the current-phase relation, which leads to a non-trivial phase shift α common to all theories discussed in this section.

5.2. *Andreev bound states in the SNS-interface*

In this section we modify the interface slightly by inserting a normal metal layer between the two superconductors. The coupling between the superconductors occurs then via quasiparticles traveling through the metal. This problem was considered many years ago by Kulik,[40] by Ishii[41] and by Bardeen and Johnson[42] for conventional superconductors. It was shown that Cooper pairs are transferred between the two superconductors via subgap bound states in the metal layer. These states are so-called Andreev bound states which are a combination of electron and Andreev-reflected hole states.[43] It is rather straightforward to understand the basic physics of this arrangement by analyzing the corresponding Bogolyubov-de Gennes (BdG) equations.

The BdG equations describe the combination of electron- and hole-like degrees of freedom in connection with the superconducting state. For a general superconductor these equations have the non-local form

$$\int d^3x' \begin{pmatrix} \left(-\frac{\hbar^2\nabla^2}{2m} - \mu\right)\delta(\boldsymbol{x}-\boldsymbol{x}') & \Delta(\boldsymbol{x},\boldsymbol{x}') \\ -\Delta^*(\boldsymbol{x},\boldsymbol{x}') & -\left(-\frac{\hbar^2\nabla^2}{2m} - \mu\right)\delta(\boldsymbol{x}-\boldsymbol{x}') \end{pmatrix} \Phi(\boldsymbol{x}') = E\Phi(\boldsymbol{x}), \tag{5·8}$$

where

$$\Phi(\boldsymbol{x}) = \begin{pmatrix} u(\boldsymbol{x}) \\ v(\boldsymbol{x}) \end{pmatrix} \tag{5·9}$$

is the spinor wave function in Nambu space with the electron-like and the hole-like components (for an elementary introduction we refer to Refs. 44) and 45)). The discussion of the wave function usually becomes simplified if we assume that only the degrees of freedom close to the Fermi level are important. One may then use the Andreev approximation, where the fast oscillating part of the wave function, proportional to $e^{i\boldsymbol{k}_F\cdot\boldsymbol{x}}$, is separated from the long-wavelength variations. The corresponding local BdG equation is

$$\begin{pmatrix} -v_F(i\hat{\boldsymbol{k}}_F \cdot \nabla - k_F) & \Delta(\hat{\boldsymbol{k}}_F, \boldsymbol{x}) \\ -\Delta^*(\hat{\boldsymbol{k}}_F, \boldsymbol{x}) & v_F(i\hat{\boldsymbol{k}}_F \cdot \nabla - k_F) \end{pmatrix} \hat{\Phi}(\hat{\boldsymbol{k}}_F, \boldsymbol{x}) = E\hat{\Phi}(\hat{\boldsymbol{k}}_F, \boldsymbol{x}), \qquad (5\cdot10)$$

where $\hat{\Phi}(\hat{\boldsymbol{k}}_F, \boldsymbol{x})$ is the spinor wave function with the components $u_{\hat{\boldsymbol{k}}_F}(\boldsymbol{x})$ and $v_{\hat{\boldsymbol{k}}_F}(\boldsymbol{x})$ for the momentum direction $\hat{\boldsymbol{k}}_F$ on the Fermi surface. Furthermore, v_F denotes the Fermi velocity k_F/m along the momentum direction $\hat{\boldsymbol{k}}_F$. In this formulation we can essentially decouple the different momentum directions.

In the following we consider a situation equivalent to that depicted in Fig. 2 with a normal metal layer of thickness L between the superconductors.[46)-48)] In order to emphasize the essential parts of the physics of this device we consider several simplifications. We assume that the band structure is the same in both superconductors and the metal and that the Fermi surface is cylindrical allowing us to neglect the c-axis in our treatment. We also do not attempt to solve the problem self-consistently, but assume the following structure of the gap as given:

$$\Delta(\hat{\boldsymbol{k}}_F, \boldsymbol{x}) = \begin{cases} \Delta_0 & -\infty < \boldsymbol{n} \cdot \boldsymbol{x} < -L/2, \\ 0 & -L/2 \leq \boldsymbol{n} \cdot \boldsymbol{x} \leq +L/2, \\ \Delta_0 e^{i\varphi} \cos(2(\vartheta_{\hat{\boldsymbol{k}}_F} - \theta) & +L/2 < \boldsymbol{n} \cdot \boldsymbol{x} < +\infty. \end{cases} \qquad (5\cdot11)$$

Here $\vartheta_{\hat{\boldsymbol{k}}_F}$ is the angle corresponding to the momentum direction $\hat{\boldsymbol{k}}_F$. We solve this BdG equation for wave functions which are continuous at the two boundaries between metal and superconductor, because we assume that the boundaries are completely transparent. Note that this last assumption is compatible with the previous simplification for band structure.

The solutions in the different regions are obtained straightforwardly by introducing the ansatz:

$$\hat{\Phi}_{\hat{\boldsymbol{k}}_F}(\boldsymbol{x}) = \begin{pmatrix} u_N \\ v_N \end{pmatrix} e^{ik\boldsymbol{n}\cdot\boldsymbol{x}} e^{i\hat{\boldsymbol{k}}_F \cdot \boldsymbol{x}} \qquad (5\cdot12)$$

for the normal metal layer and

$$\hat{\Phi}_{\hat{\boldsymbol{k}}_F}(\boldsymbol{x}) = \begin{pmatrix} u_{S,D} \\ v_{S,D} \end{pmatrix} e^{-\kappa_{S,D}|\boldsymbol{n}\cdot\boldsymbol{x}|} e^{i\hat{\boldsymbol{k}}_F \cdot \boldsymbol{x}} \qquad (5\cdot13)$$

for the two superconductors, where S and D denote the s-wave and the d-wave side, respectively. Note, that with our assumption we restrict ourselves to $k, \kappa \ll k_F$ such that we can consider the quasiparticles and holes as traveling essentially along the direction $\hat{\boldsymbol{k}}_F$. Therefore the upper component of $\hat{\Phi}_{\hat{\boldsymbol{k}}_F}(\boldsymbol{x})$ in Eq. (5·12)

describes an electron moving along $\hat{\boldsymbol{k}}_F$, while the lower component corresponds to the Andreev reflected hole in opposite direction. The exponentially decaying solution in the superconducting regions (Eq. (5·13) requires that the energy of the state is lower than both of the gap values in the two directions. We concentrate here on only these types of states, which yield bound states in the normal metal region, and we discard all states which are extended as Bogolyubov quasiparticles in either of the superconductors. The solutions are matched at the boundaries $\boldsymbol{n} \cdot \boldsymbol{x} = \pm L/2$. This yields the eigenvalue equation for the subgap bound states,

$$\frac{2EL}{|v_n|} - \arccos\left(\frac{E}{|\Delta_0|}\right) - \arccos\left(\frac{E}{|\Delta_{\hat{\boldsymbol{k}}_F}|}\right) = 2\pi n + \operatorname{sgn}(\hat{\boldsymbol{k}}_F \cdot \boldsymbol{n})\tilde{\varphi}, \tag{5·14}$$

where $\Delta_{\hat{\boldsymbol{k}}_F} = \Delta_0 \cos(2(\vartheta_{\hat{\boldsymbol{k}}_F} - \theta))$ is the direction dependent d-wave gap function and $\tilde{\varphi}$ is the phase difference between the two superconductors with the definition

$$\tilde{\varphi} = \begin{cases} \varphi & \Delta_{\hat{\boldsymbol{k}}_F} > 0, \\ \varphi + \pi & \Delta_{\hat{\boldsymbol{k}}_F} < 0 \end{cases} \tag{5·15}$$

and $v_n = \hat{\boldsymbol{k}}_F \cdot \boldsymbol{n} k_F/m$.

We now consider the case of L large compared with the coherence length ξ_0 in both superconductors so that the number of subgap bound states is very large. The energies of the states close to the Fermi level are then given by the simple form

$$E_n(\hat{\boldsymbol{k}}_F) = \frac{\hbar^2 k_F}{2mL_{\hat{\boldsymbol{k}}_F}}[(2n+1)\pi + \operatorname{sgn}(\hat{\boldsymbol{k}}_F \cdot \boldsymbol{n})\tilde{\varphi}], \tag{5·16}$$

where $L_{\hat{\boldsymbol{k}}_F} = L/|\hat{\boldsymbol{k}}_F \cdot \boldsymbol{n}|$ is the traveling distance of the electron or hole in the normal metal. We assume here that the metal is in the clean limit, so that we need not concern ourselves with impurity scattering effects.

First we analyze the lowest energy configuration of the junction. For this purpose we consider the free energy density contribution of the Andreev bound states,

$$F = -k_B T \int_{-\pi/2}^{+\pi/2} d\vartheta_{\hat{\boldsymbol{k}}_F} \frac{k_F}{L_{\hat{\boldsymbol{k}}_F}} \sum_{s=\pm 1} \sum_{n=-\infty}^{+\infty} \ln\left[1 + \exp\left\{-\beta \frac{\hbar^2 v_F}{2L_{\hat{\boldsymbol{k}}_F}}\{(2n+1)\pi + s\tilde{\varphi}(\vartheta_{\hat{\boldsymbol{k}}_F})\}\right\}\right] \tag{5·17}$$

with the approximation that Eq. (5·16) is valid for all n, which gives good results for $k_B T \ll \Delta_0$. This free energy is an even 2π-periodic function of φ.[48] Therefore we may expand it in terms of $\cos(n'\varphi)$ as

$$F = \sum_{n'=0}^{\infty} \int_{-\pi/2}^{+\pi/2} d\vartheta_{\hat{\boldsymbol{k}}_F} f_{n'}(\vartheta_{\hat{\boldsymbol{k}}_F}) \cos(n'\varphi), \tag{5·18}$$

where

$$f_{n'}(\vartheta_{\hat{\boldsymbol{k}}_F}) = \frac{k_B T k_F}{n' L_{\hat{\boldsymbol{k}}_F}} \frac{[-\mathrm{sgn}(\cos(2(\vartheta_{\hat{\boldsymbol{k}}_F} - \theta)))]^{n'}}{\sinh(n' L_{\hat{\boldsymbol{k}}_F}/\xi(T))} \tag{5·19}$$

with $\xi(T) = \hbar v_F / 2\pi k_B T$ corresponding to the coherence length in the normal metal. Analogous to the previous section, the terms with $n' > 1$ are interpreted as representing multiple (n'-fold) Cooper transfer, or, in this case, multiple Andreev scattering. [46)-48)]

In view of the fact that the coefficients $f_{n'}$ fall off exponentially fast with increasing n', we may discard all orders with $n' > 2$. We then obtain a form for F as in Eq. (5·2). We can then discuss the minimizing phase difference φ which corresponds again to the intrinsic phase shift. For the special case $\theta = \pm\pi/4$ (the nodes of the d-wave pair wave function point towards the interface), the coefficients with odd n' disappear, and the even-n' coefficients are positive. Thus, the minimal free energy is attained at $\varphi = \pm\pi/2$ for all temperatures. This result is identical to that reached in the previous section. For deviating angles θ, the phase shift is in general different and depends on temperature. It is also possible to draw the corresponding phase diagram, as shown in Fig. 4, based on the free energy in Eq. (5·18).

What is the origin of this instability towards a time-reversal symmetry breaking state here? An important property of Eq. (5·16) is the existence of zero-energy states, for phase differences of $\tilde{\varphi} = \pm\pi$ independent of the angle $\vartheta_{\hat{\boldsymbol{k}}_F}$. These states generate a finite density of states at zero energy. The single quasiparticle density of states for small energies is defined as

$$\rho(\omega) = \int \frac{d\vartheta_{\hat{\boldsymbol{k}}_F}}{2\pi} \frac{k_F}{L_{\hat{\boldsymbol{k}}_F}} \sum_n \delta(\omega - E_n(\hat{\boldsymbol{k}}_F)). \tag{5·20}$$

For the sake of simplicity, we evaluate this expression only for the case $\theta = \pi/4$, and we obtain for $\omega > 0$

$$\rho(\omega) = \frac{2k_F}{\pi L} \sum_{n=-\infty}^{+\infty} \sum_{s=\pm 1} \mathrm{Re}\left[\frac{|\omega|}{\Omega_{n,s}\sqrt{\Omega_{n,s}^2 - \omega^2}}\right] \Theta(\Omega_{n,s}), \tag{5·21}$$

where $\Omega_{n,s} = \frac{\hbar^2 v_F}{2L}(n\pi - s\varphi)$, and Θ is the step function. The factor 2 is necessary to account for the two spin states per quasiparticle level. Note that this form is only valid for ω small compared with the gap size. In the form of $\rho(\omega)$ we recognize the structure of discrete levels (Fig. 5(a)) due to the finite width of the normal metal layer. In addition to the

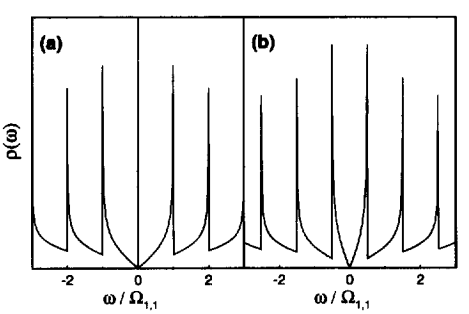

Fig. 5. Density of states of the Andreev levels in the SND interface for the angle $\theta = \pi/4$. a) The phase difference φ is fixed at 0 or π with a peak at $\omega = 0$. b) The phase difference φ is $\pi/4$ with a pseudogap feature corresponding to the lowest energy state of the device.

square root singularity of each level, we find a tail extending in the direction of decreasing ω. In the limit of vanishing ω (below the lowest discrete level structure), this leads to a suppression of $\rho(\omega)$ linear in ω. For the cases $\varphi = 0$ and π, we find in addition a δ-peak at $\omega = 0$ which contains the weight of the zero-energy bound states,

$$\lim_{\varepsilon \to 0} \int_0^{\varepsilon} d\omega \rho(\omega) = \frac{2k_F}{\pi L} \neq 0. \tag{5·22}$$

Thus the driving element for the time-reversal symmetry breaking state is the local Fermi surface instability, i.e., the removal of the zero-energy bound states from the Fermi level. The zero-energy level splits into two as soon as $\varphi \neq 0$ and π, one below and one above the Fermi level. This splitting which corresponds to a gap-like feature is largest for $\varphi = \pm\pi/2$ in the case $\theta = \pi/4$ (Fig. 5(b)). The opening of a gap in the quasiparticle spectrum is the essential point in stabilizing the time reversal symmetry breaking state.

We turn now to the Josephson current which can be obtained via the derivative of the free energy with respect to φ. We can separate the current contribution for each $\hat{\boldsymbol{k}}_F$:

$$\boldsymbol{J}_{\hat{\boldsymbol{k}}_F} = -\frac{2e\hat{\boldsymbol{k}}_F}{\hbar} L_{\hat{\boldsymbol{k}}_F} \left.\frac{dF}{d\varphi}\right|_{\hat{\boldsymbol{k}}_F} = \frac{2e\hat{\boldsymbol{k}}_F}{\hbar} L_{\hat{\boldsymbol{k}}_F} \sum_{n'=0}^{\infty} n' f_{n'}(\vartheta_{\hat{\boldsymbol{k}}_F}) \sin(n'\varphi). \tag{5·23}$$

This allows us to easily decompose the current into the perpendicular component, $J_\perp$, passing through the junction (Josephson current) and the component parallel to the metal layer, $J_\parallel$,[48]

$$\begin{pmatrix} J_\perp \\ J_\parallel \end{pmatrix} = \frac{2ek_F}{\hbar} \int_{-\pi/2}^{+\pi/2} \frac{d\vartheta_{\hat{\boldsymbol{k}}_F}}{2\pi} L_{\hat{\boldsymbol{k}}_F} \sum_{n'=0}^{\infty} \begin{pmatrix} \cos\vartheta_{\hat{\boldsymbol{k}}_F} \\ \sin\vartheta_{\hat{\boldsymbol{k}}_F} \end{pmatrix} n' f_{n'}(\vartheta_{\hat{\boldsymbol{k}}_F}) \sin(n'\varphi). \tag{5·24}$$

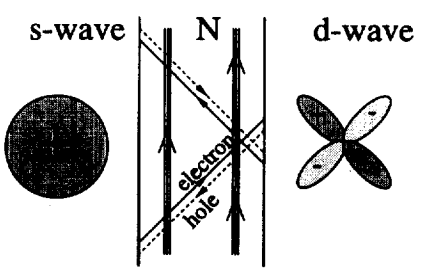

Fig. 6. Current structure in the SND junction. The Andreev bound states carry quasiparticle current between the s-wave and d-wave superconductors. While the current component from s- to d-wave superconductors is canceled exactly, there is a finite component along the normal metal layer N.

The lowest energy state is obviously given by $J_\perp(\varphi = \varphi_0) = 0$. The vanishing of $J_\perp$ implies the overall cancelling of all current contributions in different $\hat{\boldsymbol{k}}_F$-directions projected on the normal vector of the normal metal layer. For $\varphi_0 \neq 0$, π, however, the parallel current component is not zero. This fact is not only clear from Eq. (5·23), but it is also intuitively easy to understand by considering the current components in Fig. 6. The presence of a finite parallel current component is a clear manifestation of broken time-reversal symmetry, since there is a degenerate state with

reversed current. In our approach this spontaneous current flows uniformly in the metal layer and for the case $\theta = \pi/4$ and $T = 0$, we find that the total current is given by[48)]

$$I_{\|} = LJ_{\|}(\varphi = \pi/2) = \frac{ek_F^2}{2\pi^2}. \tag{5·25}$$

(Note that this expression is valid for two dimensions only, because we have neglected the motion of quasiparticles along the c-direction.) The current $I_{\|}$ is independent of the width L (for any angle θ). This result is only correct in the clean limit, where the mean free path of the quasiparticles is much longer than L. The number of bound states increases proportionally to L. Simultaneously, however, the current carried by each bound state decreases with L^{-1} so that the width does not enter in the total current. For finite temperatures the coherence length $\xi(T)$ sets an upper bound on L for which $I_{\|}$ is independent of L.[48)]

5.3. *Ginzburg-Landau treatment for SNS-interface*

In this section we consider the SNS-interface on the phenomenological level assuming that the s-wave and d-wave order parameter coexist in the normal metal layer due to the proximity effect from the two superconductors.[49)] The formulation of this problem based on the generalized Ginzburg-Landau theory allows us to also treat the spatial dependence of the order parameter simultaneously with the static magnetic properties, including the spontaneous currents seen in the previous subsection and related screening effects.

We use the most general free energy expansion in the two order parameters η_s and η_d:

$$\begin{aligned}\frac{\mathcal{F}}{f_0} = \int d^3r \Bigg[& \sum_{\mu=s,d} \left\{ \left(\frac{T}{T_{c\mu}(\boldsymbol{x})} - 1 \right) |\eta_\mu|^2 + \beta_\mu |\eta_\mu|^4 + \xi_\mu^2 |\boldsymbol{\Pi}_\mu|^2 \right\} \\ & + \gamma_1 |\eta_s|^2 |\eta_d|^2 + \frac{\gamma_2}{2} (\eta_s^{*2} \eta_d^2 + \eta_s^2 \eta_d^{*2}) \\ & + \tilde{\xi}^2 ((\Pi_x \eta_s)^* (\Pi_x \eta_d) - (\Pi_y \eta_s)^* (\Pi_y \eta_d) + \text{c.c.}) + \frac{(\nabla \times \boldsymbol{A})^2}{8\pi f_0} \Bigg], \end{aligned} \tag{5·26}$$

where f_0 is a free energy density, and T_{cs} and T_{cd} are the transition temperatures of η_s and η_d, respectively, and $\beta_{s,d}$, $\gamma_{1,2}$, $\xi_{s,d}$ and $\tilde{\xi}$ are real coefficients ($\xi_{s,d}$ corresponds to the zero-temperature coherence length in the superconductors). For the gradients we write $\boldsymbol{\Pi} = \nabla - (2\pi i/\Phi_0)\boldsymbol{A}$, with vector potential $\boldsymbol{A}$ and flux quantum $\Phi_0 = hc/2e$. The coordinates used in the free energy are those of the d-wave superconductor. This fact is important for the mixed gradient term.

The free energy has in general a different form in the three regions. For simplicity we assume that the electronic properties are the same in all three regions apart from the pairing interaction which leads to s-wave and d-wave superconductivity and normal metal behavior, respectively. Therefore, all coefficients in $\mathcal{F}$ are constant, and only the critical temperatures depend on position. We take $T_{cs(d)} > 0$ in the

$s(d)$-wave superconductor and zero otherwise. We also ignore the spatial dependence along the c-direction so that we can restrict our discussion to the xy-plane. By considering an infinite SNS-interface, the problem reduces to one dimension, and all spatial dependence of the order parameters and the vector potential is only along the interface normal vector $\boldsymbol{n}$. These simplifications do not affect the essential physical properties we discuss below.

The properties of the SNS-interface are now obtained by the variation of the free energy with respect to η_s, η_d and $\boldsymbol{A}$. In analogy to the previous study we assume the complete transparency of the NS-interfaces, so that the order parameter is continuous there. In the normal metal layer and in its immediate vicinity the s- and d-wave order parameters coexist due to the proximity effect, and they have to be combined in some way. Most interesting for us is the relative phase between them, because it is again related with the Josephson effect through the interface.

There are two terms in the free energy which determine the relative phase $\varphi_0 = \phi_s - \phi_d$. The first one is the fourth-order term,

$$\frac{\gamma_2}{2}(\eta_s^{*2}\eta_d^2 + \eta_s^2\eta_d^{*2}) = \gamma_2|\eta_s|^2|\eta_d|^2\cos(2\varphi_0) \tag{5·27}$$

which favors $\varphi_0 = 0, \pi$ for $\gamma_2 < 0$ and $\varphi_0 = \pm\pi/2$ for $\gamma_2 > 0$. If the free energy is derived from a generic microscopic model allowing the coexistence of s- and d-wave order parameters, then $\gamma_2 > 0$ is found in the weak coupling approach. The reason for this is that the state with $\varphi_0 = 0$ or π has, in general, nodes in the gap (they are shifted with respect to the [110]-direction), while for $\varphi_0 = \pm\pi/2$ the nodes are removed, as mentioned above. The nodeless state is energetically favored as it gains more condensation energy by moving quasiparticle states away from the Fermi energy. Therefore we continue assuming that γ_2 is positive.

The other term involved in determining the relative phase is the second-order mixing gradient term,

$$\tilde{\xi}^2[(\partial_x\eta_s^*)(\partial_x\eta_d) - (\partial_y\eta_s^*)(\partial_y\eta_d) + \text{c.c.}] = \tilde{\xi}^2(n_x^2 - n_y^2)[(\partial_n\eta_s^*)(\partial_n\eta_d) + \text{c.c.}], \tag{5·28}$$

where we have neglected the vector potential (∂_n is the derivative along the normal vector $\boldsymbol{n}$). Obviously, this term is effective only if the order parameter varies in space, i.e. mainly in the region of the normal metal layer. The relative phase preferred here is $\varphi_0 = 0$ if $n_x > n_y$ and $\varphi_0 = \pi$ if $n_y > n_x$. It is this term which mediates the (lowest order) Josephson coupling between the two superconductors. This becomes clear if we write it in the following form neglecting any spatial variation of the order parameter phases: $\tilde{\xi}^2\cos(2\theta)(\partial_n|\eta_s|)(\partial_n|\eta_d|)\cos\varphi$ (note that $\cos(2\theta) = n_x^2 - n_y^2$).

The relative phase obtained from minimization of $\mathcal{F}$ corresponds to the intrinsic phase shift in the Josephson effect. Thus the second-order term in Eq. (5·28) creates the distinction between a 0- and a π-junction. If the orientation angle, θ, is $\pi/4$ this term is ineffective, so that the fourth-order term in Eq. (5·27) fixes φ_0 to be $\pm\pi/2$ which is a time-reversal symmetry breaking state, as found above. Here now we have indeed a region around the normal metal where the superconducting state forms a time-reversal symmetry breaking state of the form $s \pm id$. This aspect was not obvious in the previous two descriptions, since there we neglected the overlap of the

order parameters due to simplifications. We realize here that the state with broken time-reversal symmetry is stabilized by the removal of the nodes in the d-wave gap in the region of the overlap. Thus this mechanism is consistent with interpretation we gave in the description using Andreev bound states. In both cases a gap has opened for the quasiparticles in the normal metal region.

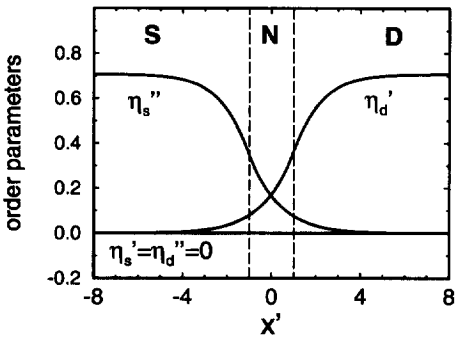

Fig. 7. Spatial dependence of the order parameter for the parameters $\beta_s = \beta_d = 1/2$, $\xi_s = \xi_d = 1$, $\gamma_1 = 2\gamma_2 = 4/5$, $\tilde{\xi} = 1$, $T_{cd} = T_{cs}$ and $T = T_{cs}/2$. The spatial axis $x' = \boldsymbol{n} \cdot \boldsymbol{x}$ is given in units of ξ_s and $\eta_\mu = \eta'_\mu + i\eta''_\mu$.

In Fig. 7 we show the numerical result of the variation of $\mathcal{F}$ for the case $\theta = \pi/4$ for a given set of parameters. In the overlapping region we indeed find a constant relative phase φ_0. As we deviate from $\theta = \pi/4$, the second order term gains importance, and the relative phase is shifted away from $\pi/2$ until it finally reaches $\varphi_0 = 0$ or π for sufficiently large angle. The second-order term tends to dominate over the fourth-order term at higher temperature, where η_s and η_d are small. Thus also here the phase diagram, θ versus temperature, has qualitatively the same form as in Fig. 4. Also here we find a second order transition line between the time-reversal invariant and the time-reversal breaking interface state.

We turn now to the magnetic properties of the time-reversal symmetry breaking interface state. As in the previous subsection, the lowest energy state is also characterized by the condition that no supercurrent flows through the interface. The current is obtained from the free energy via the London (Maxwell) equation. The variation with respect to the vector potential leads to

$$\frac{1}{4\pi}\nabla \times (\nabla \times \boldsymbol{A}) = -\frac{\partial \mathcal{F}}{\partial \boldsymbol{A}} = \frac{1}{c}\boldsymbol{J}. \tag{5·29}$$

This leads to the current passing through the interface,

$$J_\perp = \sum_{\mu=s,d} \xi_\mu^2 \left[\frac{4\pi c}{\Phi_0}\mathrm{Im}(\eta_\mu^* \partial_n \eta_\mu) - \frac{8\pi^2 c}{\Phi_0^2}|\eta_\mu|^2 \boldsymbol{n}\cdot\boldsymbol{A}\right]$$
$$-\frac{2\pi c\tilde{\xi}^2}{\Phi_0}(n_x^2 - n_y^2)\mathrm{Im}(\eta_s^* \partial_n \eta_d - \eta_d \partial_n \eta_s^*) - \frac{8\pi^2 c\tilde{\xi}^2}{\Phi_0^2}(\eta_s^* \eta_d + \eta_s \eta_d^*)(n_x A_x - n_y A_y) \tag{5·30}$$

and the current parallel to the metal layer (within the xy-plane),

$$J_{\parallel} = \frac{8\pi^2 c}{\Phi_0^2} \sum_{\mu=s,d} \xi_\mu^2 |\eta_\mu|^2 (A_y n_x - A_x n_y)$$

$$+ \frac{2\pi\tilde{\xi}^2 c}{\Phi_0} n_x n_y \mathrm{Im}(\eta_s^* \partial_n \eta_d - \eta_d \partial_n \eta_s^*) - \frac{8\pi^2 \tilde{\xi}^2 c}{\Phi_0^2} (\eta_s^* \eta_d + \eta_s \eta_d^*)(A_x n_y + A_y n_x). \tag{5·31}$$

In this case the vanishing of $J_\perp$ occurs as the cancelling of the paramagnetic and diamagnetic parts and is, in general, not easy to analyze using Eq. (5·30).[33),49),51)] For $J_\parallel$, the paramagnetic part originating exclusively from the mixing gradient term creates a finite current if time-reversal symmetry is broken in the region where the order parameter varies in space. The mixing gradient term with its $x^2 - y^2$-form yields a similar angular structure for the currents as the Andreev bound states did in the previous subsection. In the case that $\theta = \pi/4$, the currents flow in opposite directions for $\vartheta > 0$ and < 0.

A current flowing in the metal layer generates a field with opposite sign on the two sides. This field is screened by diamagnetic counter currents in the superconductor on a length scale $\lambda_L \approx \Phi_0/\sqrt{32\pi^3 c \xi_\mu |\eta_\mu|}$, the London penetration depth. Numerical data regarding the current and field distribution are displayed in Fig. 8.

The description in terms of Ginzburg-Landau theory has been given in various ways. The idea of a proximity effect leading to an overlap of s-wave and d-wave order parameters can also be applied even in the absence of a normal metal layer and leads essentially to the same results.[49)] Furthermore, lattice defects such as dislocations can also generate locally time-reversal symmetry breaking states in a d-wave superconductor.[50)] In this case an additional order parameter component is introduced in the vicinity of the defect. This effect occurs also if one assumes a whole line of dislocations, which then behaves in many respects very similarly to the SNS-interface, as shown in Ref. 51).

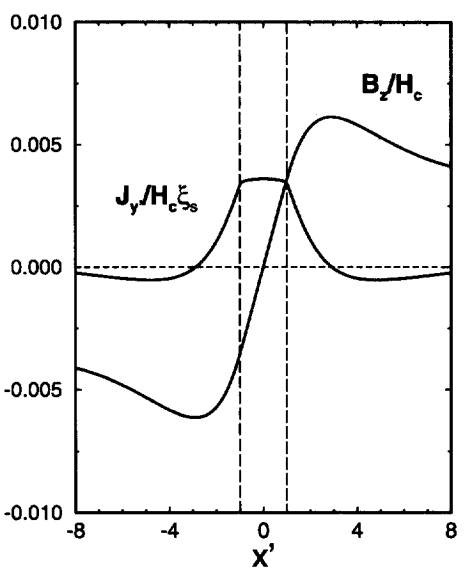

Fig. 8. Current and magnetic field distribution at the SND interface. The parameters are the same as in Fig. 7. In addition we fix $\Phi_0/2\sqrt{2}\pi H_c \xi_s^2 = 4$, which corresponds to the London penetration depth in units of ξ_s.

The three ways of describing the interface between an s-wave and a d-wave superconductor close to the critical angle $\theta = \pi/4$ create a consistent and complementary picture. The presence of several order parameters makes it possi-

ble to generate a time-reversal symmetry breaking state. In the second and third model we have seen that the driving mechanism for such a state is the opening of a gap in the quasiparticle spectrum. For this purpose it is necessary that there are low lying quasiparticle excitations. The d-wave provides such states because of its phase structure which leads to nodes in the gap. Therefore we do not expect that a conventional s-wave superconductor would generate a similar effect.

§6. Consequences of broken time-reversal symmetry on a Josephson junction

Various physical phenomena appear in connection with the time-reversal breaking state on the Josephson junction or SNS-interface. The presence of spontaneous currents and magnetic fields is one of the most direct manifestations of such a state. From our previous discussion, however, it is clear that the resulting magnetization does not lead to a net magnetic moment of the system, and the field distribution actually extends only over about the London penetration depth. Hence, only a very sensitive probe with high spatial resolution would be able to detect these fields. Furthermore, it occupies only a small fraction of the whole sample. Other consequences of broken time-reversal symmetry could, therefore, also be more easily accessible for experimental verification. We discuss here two effects which seem to be most promising. The first is the possibility of fractional flux quanta,[32),33),49),52),53)] and the second is connected with phase slips[51)] between the two degenerate junction states.

6.1. *Fractional flux quanta*

We consider a long homogeneous Josephson junction. The phase difference φ is, in general, not uniform, but can vary over a certain length scale λ_J (Josephson penetration depth), the screening length for external magnetic fields in the junction. A Josephson junction can also support flux lines (vortices) which contain fluxes $\Phi = n\Phi_0$ like standard vortices. These vortices are most conveniently described through the spatial variation of φ along the junction. For the following we consider a junction which lies in the x-z-plane with the direction of the magnetic field along the z-axis and the variation of φ exclusively along x. A varying phase difference φ corresponds to the presence of a local magnetic field b_z,

$$\frac{\partial \varphi}{\partial x} = \frac{2\pi}{\Phi_0}(2\lambda_L + d)b_z \tag{6·1}$$

with d as the width of the junction.[16)] Note that b_z is the field averaged in the direction perpendicular to the junction such that $(2\lambda_L + d)b_z$ is the local magnetic flux density. Using Maxwell's equations and the Josephson current-phase relation, $\partial b_z/\partial x = 4\pi J/c = (4\pi/c)J_c \sin\phi$, we obtain the sine-Gordon equation,

$$\frac{\partial^2 \varphi}{\partial x^2} = \frac{1}{\lambda_J^2}\sin\varphi, \tag{6·2}$$

where $\lambda_J = \sqrt{c\Phi_0/8\pi^2 J_c(2\lambda_L + d)}$. This equation gives a proper description of the junction properties in the limit $\lambda_L \ll \lambda_J$.[16] Obviously, the constant solutions $\varphi = 2\pi n$ are stable.

A vortex corresponds to a kink (width $\sim \lambda_J$) of φ which changes between two constants $\varphi(x_1) = 2\pi n_1$ and $\varphi(x_2) = 2\pi n_2$, where $x_{1,2}$ are points far from the kink position. The enclosed flux can be calculated immediately by

$$\begin{aligned}\Phi &= \int_{x_1}^{x_2} dx(2\lambda_L + d)b_z = \frac{\Phi_0}{2\pi}\int_{x_1}^{x_2} dx\frac{\partial\varphi}{\partial x} \\ &= \frac{\Phi_0}{2\pi}[\varphi(x_2) - \varphi(x_1)] = \Phi_0(n_2 - n_1). \end{aligned} \tag{6·3}$$

The quantization is a consequence of the existence of a discrete set of stable constant-φ solutions and the magnitude of their separation. A modification of the quantization is expected as soon as other stable constant values for φ appear, such as $\varphi = \pi(2n + 1)$, i.e., a π-junction, or $\varphi = \chi + 2\pi n$ with χ arbitrary. We consider first an infinite junction which is a 0-junction for $x < 0$ and a π-junction for $x > 0$. In this case the behavior of φ is obtained from Eq. (6·2) if we replace the right-hand side by $\lambda_J^{-2}\sin(\varphi - \varphi_0)$ with $\varphi_0(x) = \pi\Theta(x)$. Under this condition the phase φ is forced to change around $x = 0$ to connect the stable solutions of φ ($= 0$ and π). The resulting kink of φ yields a flux

$$\Phi = \frac{\Phi_0}{2\pi}[\varphi(+\infty) - \varphi(-\infty)] = \Phi_0\left(n + \frac{1}{2}\right), \tag{6·4}$$

i.e., half-integer quantization, as mentioned above.[11),12)]

In the case of a time-reversal symmetry breaking state at the Josephson junction we can consider the following case of domain formation due to the two-fold degeneracy: $\varphi_0 = \chi\mathrm{sign}(x)$. As in the case discussed above, the phase φ must form a kink near $x = 0$ in order to match the conditions on both sides. Obviously, there appears a new flux quantization

$$\Phi = \Phi_0\left(n + \frac{\chi}{\pi}\right), \tag{6·5}$$

which is shifted by a junction-specific value and is neither integer nor half-integer.[32),33),54)] This type of "fractional" quantization occurs also at locations where the properties of the junctions are modified abruptly, for example, if the orientation of the interface changes (i.e., at a corner of an interface). Then also the intrinsic phase shift should assume a different value, and a fractional vortex should occur as well.

In the following we give a simple argument for the fact that the observation of anomalous flux quantization (Eq. (6·5)) is uniquely connected with the (at least local) violation of time-reversal symmetry of the superconducting state.[53)] Let us assume that a vortex with flux Φ is located somewhere on the junction. If we apply the time-reversal operation to this system, then the flux of the vortex changes sign: $\Phi \to -\Phi$. These two flux values can only differ by an integer multiple of Φ_0 if

the underlying superconducting state is not altered by this operation (apart from inverting the phase winding): i.e.,

$$\Phi = -\Phi + \Phi_0 n. \tag{6·6}$$

This leads to $\Phi = \Phi_0 n/2$, and only integer and half-integer flux values are allowed to appear. On the other hand, if the superconducting state changes under the time-reversal operation (i.e., it violates time-reversal symmetry), then no constraint is imposed on the difference between Φ and $-\Phi$, and any value of Φ is possible.

The measurement of flux quantization of this kind requires a long homogeneous junction, exceeding λ_J by many times, to confine the flux completely or to separate different flux lines sufficiently. If different flux lines overlap, then no clear evaluation of fluxes associated with each of them is possible. The observation of flux lines with fractional flux was reported some time ago on grain boundaries of a YBCO film. The sample was a *c*-axis textured film and had a triangular inclusion with a 45° misalignment of the crystal axes relative to the surrounding. Some edges of the triangle provided nearly optimal conditions for the occurrence of locally broken time-reversal symmetry according to the above discussion. The appearance of fractional fluxes on the corners and occasionally on the edges, observed by a scanning SQUID microscope, was indeed entirely consistent with the ideas presented above.[55] Nevertheless, these data have to be considered with caution, since the grain boundaries are by no means ideally homogeneous. Indeed, other experiments on so-called asymmetric 45° grain boundaries show considerable inhomogeneity which leads to remarkable fluctuations of φ along the interface and, consequently, to an observable random flux pattern.[56] Therefore it is unclear at present whether the interpretation of the above experiment in terms of broken time-reversal symmetry is appropriate.

6.2. *Modified phase slip behavior*

An effect which does not require long inhomogeneous junctions is related to a kink of φ in time. This effect, known as *phase slip*, implies that for standard Josephson junctions the phase difference φ "jumps" by a value 2π from one stable state to another. This corresponds to the passage of one standard vortex through the junction. Note, that a "π-junction" behaves in this respect in the same way.

The situation can be altered, however, when the junction violates time-reversal symmetry, because the number of stable states is doubled (additional two-fold degeneracy). Therefore a transition between stable junction states now includes also differences smaller than 2π. The transferred flux correspondingly has a fractional value in the previously defined sense. Let us assume again the simplified energy form given in Eq. (5·2), which shows a doubling of the minima in case that $|I_1/2I_2| < 1$ and $I_2 < 0$. A sufficiently large current applied in the proper direction can lead to a transition between two neighboring minima. During this process, φ varies in time and yields a voltage $V(t) = (\Phi_0/2\pi)\partial\varphi/\partial t$. The voltage signal integrated over time is related to the magnitude of the transferred flux and the total change of φ,

$$\int_{-\infty}^{+\infty} dt V(t) = \frac{\Phi_0}{2\pi}\int_{-\infty}^{+\infty} dt \frac{\partial\varphi}{\partial t} = \frac{\Phi_0}{\pi}\chi \tag{6·7}$$

and is essentially the fractional flux introduced in Eq. (6·5).[51]

Another related aspect, more easily probed experimentally, is the fact that energy is absorbed by this process, since the flow of the current is accompanied by the creation of a voltage. The barrier between two degenerate minima in the time-reversal symmetry breaking state is particularly low, close to the transition to this state. Therefore near this transition it is possible to induce oscillating phase slips between two minima by microwave radiation. The transition would be accompanied by the enhancement of the microwave absorption in the junction.[57]

Beyond these two effects, also the arrangement of energy levels of the quasiparticle bound states could indicate the violation of time-reversal symmetry. We address this issue briefly in connection with surface states, where actual experimental results seem to indicate the presence of a surface state with broken time-reversal symmetry.

§7. Surface states with broken time-reversal symmetry

This section is devoted to the discussion of the region close to the surface of a $d_{x^2-y^2}$-wave superconductor where states with broken time-reversal symmetry can also appear. We will find obvious parallels to the situation at the interface, but also several distinguishing aspects. While at an interface between two superconductors there naturally exist two order parameters (one of each side) which can form together the time-reversal symmetry breaking state,[49] only one order parameter component is a priori available close to the surface. Pair breaking effects can destroy the $d_{x^2-y^2}$-wave order parameter at the surface, however, and open the way for an order parameter of different symmetry which is suppressed in the bulk, e.g., an s-wave or d_{xy}-wave. Then this new pairing component can form a complex combination together with the dominant $d_{x^2-y^2}$-wave component.[32),33),58)-60)] Analogous to the interface, such a state is accompanied by spontaneous currents at the surface. In the following we discuss this state phenomenologically, based on a GL-theory, and microscopically, using BdG equations.

7.1. *The Ginzburg-Landau formulation*

The conditions for the appearance of a time reversal symmetry breaking state at the surface can be examined most easily using the generalized GL-theory for a $d_{x^2-y^2}$-wave and an s-wave order parameter, as introduced earlier (Eq. (5·26)). The superconductor is assumed to fill a half-space with a surface facing the [110]-direction. This is the direction where maximal pair breaking effects occur for a $d_{x^2-y^2}$-wave superconductor with a specularly reflecting surface. We assume that $T_{cd} > T_{cs} > 0$. Otherwise, all conditions presented in §5 apply here as well.

The pair breaking effects can be included in the boundary conditions which take the form

$$\left(\boldsymbol{n}\cdot\boldsymbol{\Pi}\eta_\mu - \frac{1}{b_\mu}\eta_\mu\right)\Big|_{\text{surface}} = 0 \tag{7·1}$$

with $\boldsymbol{n} = (1,1,0)$. Using $\eta_\mu = |\eta_\mu|e^{i\phi_\mu}$ we can separate the real and imaginary part

$$\left(\boldsymbol{n}\cdot\nabla-\frac{1}{b_\mu}\right)|\eta_\mu|\Big|_{\text{surface}}=0,$$
$$\boldsymbol{n}\cdot\left(\nabla\phi_\mu-\frac{2\pi}{\Phi_0}\boldsymbol{A}\right)|\eta_\mu|\Big|_{\text{surface}}=0. \tag{7·2}$$

The first equation describes the effect of surface scattering on the order parameter, while the second one represents the natural condition that no current flows perpendicular through the surface in or out of the superconductor. The parameter b_μ is the extrapolation length of the order parameter (see in Ref. 22)). For simplicity we assume $b_d=0$ and $b_s=\infty$, which implies that $|\eta_d|=0$ at the surface and η_s is not unaffected. Ignoring the s-wave component for the moment and solving the problem for η_d we find,

$$|\eta_d|(\boldsymbol{x}\cdot\boldsymbol{n})=\eta_0\tanh\left(\frac{\boldsymbol{x}\cdot\boldsymbol{n}}{\tilde{\xi}_d}\right), \tag{7·3}$$

with $\eta_0^2(T)=(1-T/T_{cd})/2\beta_d$ and $\tilde{\xi}_\mu(T)=\xi_\mu/\sqrt{1-T/T_{cd}}$.

This solution can be unstable against the admixture of the s-wave order parameter. In order to examine this possibility we consider the GL-equation linearized in η_s ($\eta_s\ll\eta_0$):

$$\left(\frac{T}{T_{cs}}-1\right)\eta_s-\xi_s^2(\boldsymbol{n}\cdot\nabla)^2\eta_s+(\gamma_1+\gamma_2\cos(2(\phi_s-\phi_d)))|\eta_d|^2\eta_s=0. \tag{7·4}$$

This equation has the form of a Schrödinger equation with a potential well defined by $|\eta_d(\boldsymbol{n}\cdot\boldsymbol{x})|^2$ and the boundary conditions. The eigenfunctions corresponding to the eigenvalue of highest temperature T describes the instability. It is easy to see that for $\gamma_2>0$ (as previously) we have to fix $\phi_s-\phi_d=\pm\pi/2$. This solution is given by $\eta_s\propto\cosh^{-\zeta}(\boldsymbol{n}\cdot\boldsymbol{x}/\tilde{\xi}_d)$, with the exponent $\zeta=\tilde{\xi}_d/\tilde{\xi}_s$. The instability temperature T^* is given by

$$\frac{T^*}{T_{cd}}=\frac{T_{cs}}{T_{cd}}\frac{1+S}{1+S\dfrac{T_{cs}}{T_{cd}}}, \tag{7·5}$$

where $S=\frac{\xi_s^2}{2\xi_d^2}\left[1-\sqrt{1+\frac{2(\gamma_1-\gamma_2)}{\beta_d}\frac{\xi_d^2}{\xi_s^2}}\right]$. Note that T^* is smaller than T_{cs} because $S<0$. It is, however, larger than the bulk transition temperature T_s^* (defined in the same way by Eq. (7·5), but with $S=-(\gamma_1-\gamma_2)/2\beta_d$) to the $s+id$-wave state.

The result of this discussion is that for temperatures below T^*, an s-wave component appears close to the surface. This component decays towards the bulk and forms a time-reversal symmetry breaking state with an $s+id$-wave form close to the surface. There are two basic conditions that this kind of state can appear: (1) the bare s-wave transition temperature must be positive, $T_{cs}>0$; (2) the coefficients γ_1 and γ_2 satisfy $\gamma_1>\gamma_2>0$. The meaning of the latter condition is that the presence

of the d-wave state suppresses the s-wave state ($T_s^* < T_{cs}$). The suppression of the d-wave component at the surface allows the s-wave component to appear. The conditions to generate a time-reversal symmetry breaking state are considerably more restrictive here than in the case of the interface.

Using Eqs. (5·31) and (5·30) we find also here a spontaneous supercurrent flowing parallel to the surface. The decay of the s-wave component and screening effects lead to the vanishing of this current in the bulk region.[33] Unlike in the case of the interface, the net magnetization need not vanish here, and we may expect macroscopically observable magnetic phenomena in principle.[52]

7.2. *The role of Andreev bound states at the surface*

In the region of the width $\sim \tilde{\xi}_d$ close to the surface where the d-wave order parameter (gap) is reduced, quasiparticle states different from those in the bulk occur. For subgap states these consist of Andreev bound states similar to those analyzed in §5. We consider a specularly reflecting surface with [110]-orientation. An Andreev bound state is created when the electron (hole) follows a trajectory which for it is reflected once at the surface (Fig. 9). Due to the symmetry, the Andreev reflections connect superconducting gaps with a phase difference π, since at one end of the trajectory the positive and on the other the negative lobe of the $d_{x^2-y^2}$-wave function is involved in the reflection process. The energies of these states are calculated practically in the same way as shown in §5. We have

$$\alpha \tilde{E} \sin\theta - \arccos(\tilde{E}) = \left(n + \frac{1}{2}\right)\pi, \tag{7·6}$$

where α is of order 1, $\tilde{E} = E/|\Delta_d(\theta)| = E/|\Delta_0 \sin 2\theta|$, $\Delta_d(\theta)$ is the angle-dependent d-wave gap, and θ is the angle with respect to the normal vector in the x-y-plane. It is easy to see that irrespective of the parameters we always find a solution with $E = 0$, i.e., we have the zero-energy bound state. This was first noticed by Hu[61),62)] and later discussed in detail by several groups.[63)-70)] Since essentially any angle θ yields such a zero-energy state, the local quasiparticle density of states at the surface has a peak at $E = 0$, similar to the situation for the SNS-interface (Fig. 5).[71)]

The admixture of an s-wave order parameter in the surface region with a relative phase $\phi_s - \phi_d = \pm\pi/2$ leads to a new phase structure encountered for the Andreev-reflected quasiparticles. This enters Eq. (7·6) basically through an additional phase shift term on the right-hand side $\pm\varphi(\theta, E) \neq 0$ and is given by the spatial dependence of $|\eta_s|$ and $|\eta_d|$. As a result, the degenerate zero-energy states split into two separate states, one above and one below the Fermi level. In this way the quasiparticle contribution to the free energy can be lowered, as seen in §5.2. Thus the removal of the large density of states is also here an important factor in the creation of a time-reversal symmetry breaking state.

The splitting of the zero-energy peak also leads to observable effects in quasiparticle tunneling. The surface density of states is observable in normal metal-superconductor (NS)-quasiparticle tunneling spectra provided that the interface between the metal and superconductor is sufficiently non-transparent.[72)] Then the bound states appear as resonances in the current-voltage (IV) characteristics. Thus

it was suggested that the zero-energy bound state leads to a so-called zero-bias anomaly in the tunneling spectrum. However, it was recently discussed by Matsumoto and Shiba[58)-60)] and later by Fogelström and coworkers[73)] that the occurrence of time-reversal symmetry breaking including the splitting of the zero-energy level should also lead to an observable modification in the spectrum.[74)] Indeed experiments on [110]-oriented NS devices with YBCO by Covington and coworkers showed that the zero-bias anomaly splits into a double peak below 4 K.[75)] This is a strong indication for the existence of a state with broken time-reversal symmetry at the surface.

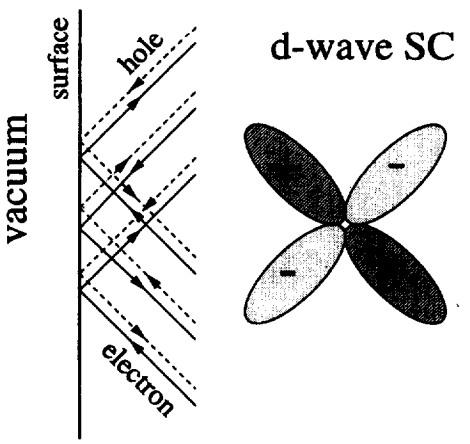

Fig. 9. Schematic view of Andreev reflection in the surface region. The drawn trajectories connect gap regions of opposite sign which lead to a phase shift π and zero-energy bound states.

It is also easy to recognize that the spontaneous currents are also carried by the quasiparticles, similar to the SNS case. The splitting of the zero-energy level leads to an imbalance in the occupation between electron states with momentum component parallel and antiparallel to $(1,-1,0)$. Thus, there is a finite current along the surface whose direction depends on which of the two degenerate time reversal symmetry breaking states is realized.[52),60)]

7.3. *Magnetic response of the surface state*

Let us now consider the magnetic properties of the surface. The fact that there is a net magnetization due to spontaneous currents gives rise to the possibility of coupling to it via an external magnetic field. This leads to an enhancement of the paramagnetic contribution above T^*, as we will show in the following. This type of effect was recently studied by Higashitani using a quasiclassical formulation.[76)] We briefly introduce the basic idea here.

The supercurrent includes two components:

$$\boldsymbol{J} = en\boldsymbol{v}_s + \boldsymbol{J}_{QP}. \tag{7·7}$$

Here, n denotes the electron density, $\boldsymbol{v}_s$ the superfluid velocity, and $\boldsymbol{J}_{QP}$ the quasiparticle contribution to the current. An external field parallel to the c-axis induces screening currents $\boldsymbol{v}_s = \frac{1}{2m}(\nabla\phi_d - \frac{2\pi}{\Phi_0}\boldsymbol{A})$ which flow parallel to the surface (parallel or antiparallel to $\boldsymbol{n}_\parallel = (1,-1,0)$) and depends on the normal coordinate $\boldsymbol{n}\cdot\boldsymbol{x}$, $\boldsymbol{v}_s = \boldsymbol{n}_\parallel v_s(\boldsymbol{n}\cdot\boldsymbol{x})$. The current $\boldsymbol{J}_{QP}$ is now given by

$$\boldsymbol{J}_{QP} = \frac{2e}{\hbar}\int_{-\pi/2}^{+\pi/2} d\vartheta_{\hat{\boldsymbol{k}}_F}\boldsymbol{v}_F\cdot\boldsymbol{n}_\parallel \int d\omega N(\omega,\vartheta_{\hat{\boldsymbol{k}}_F},\boldsymbol{n}\cdot\boldsymbol{x})f(\omega+u(\vartheta_{\hat{\boldsymbol{k}}_F},\boldsymbol{n}\cdot\boldsymbol{x})), \tag{7·8}$$

where $N(\omega, \vartheta_{\hat{\boldsymbol{k}}_F}, \boldsymbol{n}\cdot\boldsymbol{x})$ is the angle-resolved local density of states. The argument of the Fermi distribution function f contains the shift of kinetic energy $u(\vartheta_{\hat{\boldsymbol{k}}_F}, \boldsymbol{n}\cdot\boldsymbol{x}) = v_s(\boldsymbol{n}\cdot\boldsymbol{x})\hbar\boldsymbol{k}_F\cdot\boldsymbol{n}_{\|}$ due to screening currents. In analogy to Eq. (5·21) the local density of states is given by

$$N(\omega, \vartheta_{\hat{\boldsymbol{k}}_F}, \boldsymbol{n}\cdot\boldsymbol{x}) = |\boldsymbol{k}_F\cdot\boldsymbol{n}|\sum_n \delta(\omega - E_n(\vartheta_{\hat{\boldsymbol{k}}_F}))R_n(\boldsymbol{n}\cdot\boldsymbol{x}), \tag{7·9}$$

where R_n is the square of the quasiparticle wave function and is normalized as $\int_0^\infty dx R_n(x) = 1$. Note that this argument applies only if the spatial dependences occur on much longer length scales than the inverse Fermi wave vector.

For conventional superconductors, the lowest quasiparticle level is close to the gap, so that the quasiparticle current is very small compared to the screening currents. In our case, however, we have a zero-energy state,

$$N(\omega, \vartheta_{\hat{\boldsymbol{k}}_F}, \boldsymbol{n}\cdot\boldsymbol{x}) = |\boldsymbol{k}_F\cdot\boldsymbol{n}|\delta(\omega)R_0(\boldsymbol{n}\cdot\boldsymbol{x}). \tag{7·10}$$

Inserting this into Eq. (7·8), we find immediately that

$$\boldsymbol{J}_{QP} = \frac{2e}{\hbar}\frac{v_F k_F}{6k_B T}(v_s R_0)(\boldsymbol{n}\cdot\boldsymbol{x}) \tag{7·11}$$

is finite and contributes in a paramagnetic way, leading to an effective enhancement of the penetrating field.

For temperatures below T^*, however, the local angle resolved density of states may be approximated by

$$N(\omega, \vartheta_{\hat{\boldsymbol{k}}_F}, \boldsymbol{n}\cdot\boldsymbol{x}) = |\boldsymbol{k}_F\cdot\boldsymbol{n}|\frac{|\omega|}{\Omega(\vartheta_{\hat{\boldsymbol{k}}_F})\sqrt{\Omega(\vartheta_{\hat{\boldsymbol{k}}_F})^2 - \omega^2}}\theta(|\Omega(\vartheta_{\hat{\boldsymbol{k}}_F})| - \omega)\tilde{R}_0(\vartheta_{\hat{\boldsymbol{k}}_F}, \boldsymbol{n}\cdot\boldsymbol{x}), \tag{7·12}$$

where Ω is the energy level of the Andreev bound state with momentum direction $\vartheta_{\hat{\boldsymbol{k}}_F}$, and $\tilde{R}_0$ is the square of the corresponding wave function (analogous to Eq. (5·21)). It is easy to see that even in the absence of screening currents there is a finite (spontaneous) quasiparticle current, as discussed above. Furthermore, a divergent linear response occurs at the transition point to the time-reversal symmetry breaking state, indicating the appearance of spontaneous surface magnetization. (For a GL-formulation of this type of effect see also Ref. 77).)

Various other structures have been studied where spontaneously broken time-reversal symmetry can occur. One example is the twin boundary in an orthorhombically distorted originally tetragonal system.[78)-80)] Another is in the vicinity of crystal lattice dislocations.[50),51)] In both cases a state with spontaneously broken time-reversal can occur locally, giving rise to various types of phenomena discussed above. We do not go into further detail on these types of structure, and, instead refer the reader to the literature.

§8. Globally broken time-reversal symmetry

While in high-temperature superconductors time-reversal symmetry breaking is probably restricted to specific regions in the samples, there are other unconventional

superconductors where time reversal symmetry is very likely violated throughout the whole material. The two best known examples are the heavy fermion superconductors UPt_3 and $U_{1-x}Th_xBe_{13}$ $(0.017 < x < 0.045)$.[81] In these compounds the specific heat indicates two consecutive phase transitions which are both attributed to superconductivity involving pairing states of different symmetry. Most theories of this double transition are based on multi-dimensional order parameters $(\eta_1, \eta_2, ...)$ whose components have different transition temperatures.[82),83] At the onset of superconductivity, the component (say η_1) with the highest T_c becomes finite, and at the second transition one or more other components (say η_2) are admixed to form a complex order parameter combination, e.g. $\eta = (|\eta_1|, \pm i|\eta_2|)$ (reviews on this problem are given for example in Refs. 22) and 84)). A further example is the recently discovered superconductor Sr_2RuO_4[85] which has a single superconducting phase transition leading to an apparently time-reversal symmetry breaking state.[86]

Let us now briefly discuss the main effect that allows us to detect broken time-reversal symmetry in these compounds, the magnetic properties.[22),83] We have seen previously that locally time-reversal symmetry breaking states can generate spontaneous currents and field distributions. In order to generate spontaneous currents in a bulk time-reversal symmetry breaking superconductor inhomogeneities of the order parameter are necessary. Inhomogeneities occur, for example, close to impurities, lattice defects due to pair breaking or around domain walls. Usually, the generated fields do not lead to net magnetic moments, and only high resolution probes are sufficient for their observation.[52),87),88] A suitable tool of this kind is provided by spin polarized muons.[89),90] When they are injected into a material, they are trapped quickly at crystallographically symmetric locations in the lattice, and their spins precess in the local static magnetic field. This field has various origins and has, in general, random values and directions if there is no magnetic order. The field distribution can then have Gaussian form,

$$\mathcal{D}(\boldsymbol{H}) = \frac{1}{\sqrt{2\pi\sigma}} \exp\left(-\frac{H^2}{2\sigma}\right), \tag{8·1}$$

where σ is the width. This distribution leads to the time dependence of the muon spin polarization along the initial direction

$$P(t) = \frac{1}{3}\left[1 + 2(1 - \gamma_\mu^2\sigma^2t^2)\exp\left(-\frac{1}{2}\gamma_\mu^2\sigma^2t^2\right)\right], \tag{8·2}$$

where γ_μ is gyromagnetic ratio of the muon.[91] The width of the distribution is the measure of the internal field. In the time-reversal symmetry breaking superconducting state, an additional contribution comes from the field distribution around each inhomogeneity. The contribution from the superconductor for a state of the form $\eta = (|\eta_1|, i|\eta_2|)$ is $\delta\sigma_{KT} \propto |\eta_1(T)||\eta_2(T)|$. We find different characteristic temperature dependences in the above discussed examples. For UPt_3[92] and $U_{1-x}Th_xBe_{13}$[93] we find below the second transition at T_c' the approximate form

$$\delta\sigma_{KT}(T) \propto |T - T_c'|^{1/2}, \tag{8·3}$$

which is dominated by the second order parameter η_2, while η_1 is already finite and has a weaker temperature dependence.[22),83)] On the other hand, if the violation of time-reversal symmetry occurs at the onset of superconductivity, as is probably the case in Sr_2RuO_4, both order parameter components have the same temperature dependence and lead to

$$\delta\sigma_{KT}(T) \propto |T - T_c| \tag{8·4}$$

close to T_c.[86)] These types of behavior are roughly consistent with the experimental data. In particular, it is an apparent fact that the internal magnetization is enhanced in connection with superconducting phase transitions in all of these materials.

Other probes similar to the previously discussed ones may be also useful here. The low temperatures required here ($T < 1\ K$) represent one drawback for these experiments as well as material problems in some cases. There is, in principle, no obstacle to perform more direct test experiments for bulk superconductivity with broken time-reversal symmetry.

§9. Conclusion

The last few years have brought various exciting developments in the field of unconventional superconductivity. The fact that unconventional superconductors can violate time-reversal symmetry (like magnets) is one of the most intriguing aspects. At first sight such states appear artificial in the symmetry classification of possible phases. It turns out, however, that such states are favorable in order to gain condensation energy. Thus, every superconducting state with nodes in the excitation gap is in some way susceptible to a phase change which breaks time-reversal symmetry in order to remove at least some of the nodes. Most weak coupling theories including multi-dimensional order parameters predict actually broken time-reversal symmetry. In high-temperature superconductors time reversal symmetry is preserved in the bulk. The main reason for this is that the order parameter is non-degenerate and would need an additional order parameter component of different symmetry, like an s-wave or d_{xy}-wave. Therefore time-reversal symmetry can only be broken if by accident one of these other components can also be stabilized. However, it looks as if these d-wave superconductors take every chance to violate time-reversal symmetry, for example at Josephson junctions, interfaces, surfaces, twin boundaries and so on, where the d-wave order parameter is vulnerable. It is clear that an s-wave superconductors which does not have nodes in the gap and is largely unaffected by disorder should not yield any sign of broken time reversal symmetry. An interesting phenomenon occurs in connection with the quasiparticle states at the interface or surface where they generate an enhanced density of states at the Fermi surface. Here, the occurrence of the time reversal symmetry breaking appears as a local Fermi surface instability. A priori there is no reason that the system should not be able to introduce alternative surface states such as inhomogeneous spin or charge density waves in order to remove the large number of states at zero energy.[94)] This is certainly a problem which has to be studied more carefully. The examples examined in the last section, UPt_3, $U_{1-x}Th_xBe_{13}$ and Sr_2RuO_4, show also that bulk time-reversal

symmetry breaking is rather common in unconventional superconductors. Thus we may expect that further unconventional superconductors very likely exhibit some of the above-mentioned phenomena, in addition to various other effects which are possible in systems displaying bulk time-reversal symmetry violation.

Acknowledgements

I would like to thank all my collaborators on this subject: D. Agterberg, D. B. Bailey, W. Belzig, Ch. Bruder, A. Furusaki, C. Honerkamp, A. Huck, Y. B. Kim, K. Kuboki, A. B. Kuklov, R. B. Laughlin, P. A. Lee, A. J. Millis, A. van Otterlo and M. E. Zhitomirsky. In particular, I would like to express my gratitude to T. M. Rice who shared many of his ideas and introduced this field to me many years ago. I benefited a great deal from discussions with Y. S. Barash, D. Brawner, R. Joynt, J. Kirtley, J. Mannhardt, A. C. Mota, M. Ogata, H. R. Ott, T. F. Rosenbaum, J. A. Sauls, H. Shiba, C. C. Tsuei, Y. Tanaka, D. van Harlingen and S. Yip.

References

1) J. G. Bednorz and K. A. Müller, Z. Phys. **B64** (1986), 189.
2) E. Dagotto, Rev. Mod. Phys. **66** (1994), 721.
3) D. J. Scalapino, Phys. Rep. **250** (1995), 329.
4) J. F. Annett, N. Goldenfeld and A. J. Leggett, *Physical Properties of High-Temperature Superconductors V*, ed. D. M. Ginsberg (World Scientific, Singapore, 1996), p. 375.
5) P. Monthoux and D. Pines, Phys. Rev. Lett. **69** (1992), 961.
6) T. Moriya, Y. Takahashi and K. Ueda, J. Phys. Soc. Jpn. **59** (1990), 2905.
7) P. W. Anderson, Science **235** (1987), 1196.
8) G. Kotliar and J. Liu, Phys. Rev. **B38** (1988), 5142.
9) The investigation of quasi-one dimensional ladder systems provide a very good understanding of this type of mechanism which results in d-wave-like pairing. For a review see E. Dagotto and T. M. Rice, Science **271** (1996), 618.
10) S. C. Zhang, Science **275** (1997), 1089.
11) V. B. Geshkenbein, A. I. Larkin and A. Barone, Phys. Rev. **B36** (1987), 235.
12) M. Sigrist and T. M. Rice, J. Phys. Soc. Jpn. **61** (1992), 4283; Rev. Mod. Phys. **67** (1995), 505.
13) M. Sigrist and T. M. Rice, Z. Phys. **B68** (1987), 9.
14) S. E. Barrett, J. A. Martindale, D. J. Durand, C. P. Pennington, C. P. Slichter, T. A. Friedmann, J. P. Rice and D. M. Ginsberg, Phys. Rev. Lett. **66** (1991), 108.
15) Z. X. Shen, D. S. Dessau, B. O. Wells, D. M. King, W. E. Spicer, A. J. Arko, D. Marshall, L. W. Lombardo, A. Kapitulnik, P. Dickinson, S. Doniach, J. Di Carlo, A. G. Loeser and C. H. Park, Phys. Rev. Lett. **70** (1993), 1553.
16) M. Tinkham, *Introduction to Superconductivity* (Mc Graw-Hill International Editions, New York, Second Edition, 1996).
17) V. B. Geshkenbein and A. I. Larkin, Pis'ma Zh. Eksp. Teor. Fiz. **43** (1986), 306 [JETP Lett. **43** (1986), 395].
18) S. Yip, O. F. De Alcantara Bonfim and P. Kumar, Phys. Rev. **B41** (1990), 11214.
19) M. B. Walker and J. Luettmer-Strathmann, Phys. Rev. **B54** (1996), 588.
20) Ch. Bruder, A. van Otterlo and G. T. Zimanyi, Phys. Rev. **B51** (1995), 12904.
21) S. Yip, Phys. Rev. **B52** (1995), 3087.
22) M. Sigrist and K. Ueda, Rev. Mod. Phys. **63** (1991), 239.
23) D. A. Wollman, D. J. Van Harlingen, W. C. Lee, D. M. Ginsberg and A. J. Leggett, Phys. Rev. Lett. **71** (1993), 2134.

24) D. A. Wollman, D. J. Van Harlingen, J. Giapintzakis and D. M. Ginsberg, Phys. Rev. Lett. **74** (1995), 797.
25) D. Brawner and H. R. Ott, Phys. Rev. **B50** (1994), 6530.
26) A. Mathai, Y. Gim, R. C. Black, A. Amar and F. C. Wellstood, Phys. Rev. Lett. **74** (1995), 4523.
27) I. Iguchi and Z. Wen, Phys. Rev. **B49** (1994), 12388.
28) J. H. Miller, Q. Y. Ying, Z. G. Zou, N. Q. Fan, J. H. Xu, M. F. Davis and J. C. Wolfe, Phys. Rev. Lett. **74** (1995), 2347.
29) C. C. Tsuei, J. R. Kirtley, C. C. Chi, L. S. Yu-Jahnes, A. Gupta, T. Shaw, J. Z. Sun and M. B. Ketchen, Phys. Rev. Lett. **73** (1994), 593.
30) C. C. Tsuei, J. R. Kirtley, M. Rupp, J. Z. Sun, A. Gupta, M. B. Ketchen, C. A. Wang, Z. F. Ren, J. H. Wang and M. Bhushan, Science **271** (1996), 329.
31) D. J. van Harlingen, Rev. Mod. Phys. **67** (1995), 515.
32) M. Sigrist, D. B. Bailey and R. B. Laughlin, Phys. Rev. Lett. **74** (1995), 3249.
33) D. B. Bailey, M. Sigrist and R. B. Laughlin, Phys. Rev. **B55** (1997), 15239.
34) S. Yip, J. Low. Temp. Phys. **91** (1993), 203.
35) V. Ambegaokar and A. Baratoff, Phys. Rev. Lett. **10** (1963), 486.
36) G. B. Arnold, L. Low. Temp. Phys. **59** (1985), 143.
37) A. Furusaki and M. Tsukada, Solid State Commun. **78** (1991), 299.
38) Y. S. Barash, A. V. Galaktionov and A. D. Zaikin, Phys. Rev. **B52** (1995), 665.
39) Y. Tanaka, Phys. Rev. Lett. **72** (1994), 3871.
40) I. O. Kulik, Sov. Phys. JETP **30** (1970), 944.
41) C. Ishii, Prog. Theor. Phys. **44** (1970), 1525.
42) J. Bardeen and J. L. Johnson, Phys. Rev. **B5** (1972), 72.
43) A. F. Andreev, Zh. Eksp. Teor. Fiz. **46** (1964), 1823 [Sov. Phys. JETP **19** (1964), 1228].
44) S. Yip, Phys. Rev. **B32** (1985), 2915.
45) Ch. Bruder, Phys. Rev. **B41** (1990), 4017.
46) A. Kadigrobov, A. M. Zagoshkin, R. I. Shekhter and M. Jonson, Phys. Rev. **B52** (1995), R8662.
47) A. M. Zagoshkin, J. of Phys. Cond. Mat. **9** (1997), L419.
48) A. Huck, A. van Otterlo and M. Sigrist, Phys. Rev. **B56** (1997), 14163.
49) K. Kuboki and M. Sigrist, J. Phys. Soc. Jpn. **65** (1996), 361.
50) A. B. Kuklov, Phys. Rev. **B52** (1995), R7002.
51) A. B. Kuklov and M. Sigrist, Int. J. Mod. Phys. **11** (1997), 1113.
52) M. Sigrist, T. M. Rice and K. Ueda, Phys. Rev. Lett. **63** (1989), 1727.
53) M. Sigrist and Y. B. Kim, J. Phys. Soc. Jpn. **63** (1994), 4314.
54) G. E. Volovik and L. P. Gor'kov, Zh. Eksp. Teor. Fiz. **88** (1985), 1412 [Sov. Phys. JETP **61** (1985), 843].
55) J. R. Kirtley, P. Chaudhari, M. B. Ketchen, N. Khare, S.-Y. Lin and T. Shaw, Phys. Rev. **B51** (1995), 12057.
56) J. Mannhart, H. Hilgenkamp, B. Mayer, Ch. Gerber, J. R. Kirtley, K. A. Moler and M. Sigrist, Phys. Rev. Lett. **77** (1996), 2782.
57) M. Sigrist, K. Kuboki, A. B. Kuklov, D. B. Bailey and R. B. Laughlin, Czech. J. Phys. **46** (1996), 3159.
58) M. Matsumoto and H. Shiba, J. Phys. Soc. Jpn. **64** (1995), 3384.
59) M. Matsumoto and H. Shiba, J. Phys. Soc. Jpn. **64** (1995), 4867.
60) M. Matsumoto and H. Shiba, J. Phys. Soc. Jpn. **65** (1996), 2194.
61) C.-R. Hu, Phys. Rev. Lett. **72** (1994), 1526.
62) C.-R. Hu, Phys. Rev. **B57** (1998), 1266.
63) Y. Tanaka and S. Kashiwaya, Phys. Rev. Lett. **74** (1995), 3451.
64) Y. Tanaka and S. Kashiwaya, Phys. Rev. **B53** (1996), 11957.
65) S. Kashiwaya, Y. Tanaka, M. Koyanagi, H. Takashima and K. Kajimura, Phys. Rev. **B51** (1995), 1350.
66) S. Kashiwaya, Y. Tanaka, M. Koyanagi and K. Kajimura, Phys. Rev. **B53** (1996), 2667.
67) L. J. Buchholtz, M. Paumbo, D. Rainer and J. A. Sauls, J. Low Temp. Phys. **101** (1995), 1079, 1099.
68) Y. Nagato and K. Nagai, Phys. Rev. **B51** (1995), 16254.
69) Y. S. Barash, H. Burkhardt and D. Rainer, Phys. Rev. Lett. **77** (1996), 4070.

70) M. B. Walker, P. Pairor and M. E. Zhitomirsky, Phys. Rev. **B56** (1997), 9015.
71) It was noticed, however, recently by Walker and coworkers that if the length scales of variation for the quasiparticle wavefunction close to the surface is of similar order as k_F^{-1}, then the energy levels and the density of states are subject to significant corrections.[70] We do not expect significant qualitative chance, if we proceed with our simplifying assumption. However, a more detailed analysis will be necessary in future to examine this point.
72) G. E. Blonder, M. Tinkham and T. M. Klapwijk, Phys. Rev. **B25** (1982), 4515.
73) M. Fogelström, D. Rainer and J. A. Sauls, Phys. Rev. Lett. **79** (1997), 281.
74) J. X. Zhu and C. S. Ting, Phys. Rev. **B57** (1998), 3038.
75) M. Covinton, M. Aprili, E. Paraoanu, L. H. Greene, F. Xu, J. Zhu and C. A. Mirkin, Phys. Rev. Lett. **79** (1997), 277.
76) S. Higashitani, J. Phys. Soc. Jpn. **66** (1997), 2556.
77) N. Ogawa, M. Sigrist and K. Ueda. J. Phys. Soc. Jpn. **61** (1992), 1730.
78) M. Sigrist, K. Kuboki, P. A. Lee, A. J. Millis and T. M. Rice, Phys. Rev. **B53** (1996), 2835.
79) M. E. Zhitomirsky and M. B. Walker, Phys. Rev. Lett. **79** (1997), 1734; Phys. Rev. **B57** (1998), 8560.
80) W. Belzig, Ch. Bruder and M. Sigrist, Phys. Rev. Lett. **80** (1998), 4285.
81) R. H. Heffner and M. R. Norman, Comments on Cond. Matt. Phys. **17** (1996), 361.
82) P. Kumar and P. Wölfle, Phys. Rev. Lett. **59** (1987), 1954.
83) M. Sigrist and T. M. Rice, Phys. Rev. **B39** (1989), 2200.
84) J. A. Sauls, Adv. Phys. **43** (1994), 113.
85) Y. Maeno, H. Hashimoto, K. Yoshida, S. Nishizaki, T. Fujita, J. G. Bednorz and F. Lichtenberg, Nature **372** (1994), 532.
86) G. M. Luke, Y. Fudamoto, K. M. Kojima, M. I. Larkin, B. Nachumi, Y. J. Uemura, Y. Maeno, Z. Mao, Y. Mori and H. Nakamura, preprint.
87) V. P. Mineev, Pis'ma Zh. Eksp. Teor. Fiz. **49** (1989), 624 [JETP Lett. **49** (1989), 719].
88) C. H. Choi and P. Muzikar, Phys. Rev. **B39** (1989), 9664.
89) A. Schenk, *Muon Spin Rotation Spectroscopy* (Hilger, London, 1985).
90) A. Amato, Rev. Mod. Phys. **69** (1997), 1119.
91) R. Kubo and T. Toyabe, in *Magnetic Resonance and Relaxation*, ed. R. Blinc (North-Holland, Amsterdam, 1967), p. 810.
92) G. M. Luke, A. Keren, L. P. Le, W. D. Wu, Y. J. Uemura, D. A. Bonn, L. Taillefer and J. D. Garret, Phys. Rev. Lett. **71** (1993), 1466.
93) R. H. Heffner, J. L. Smith, J. O. Willis, P. Birrer, C. Baines, F. N. Gygax, B. Hitti, E. Lippelt, H. R. Ott, A. Schenk, E. A. Knetsch, J. A. Mydosh and D. E. MacLaughlin, Phys. Rev. Lett. **65** (1990), 2816.
94) For a related effect in a non-superconductor see, M. Fujita, K. Wakabayashi, K. Nakada and K. Kusakabe, J. Phys. Soc. Jpn. **65** (1996), 565.